Hindawi
International Journal of Aerospace Engineering
Volume 2024, Article ID 1850204, 8 pages
https://doi.org/10.1155/2024/1850204

Research Article

The Channel Fading Influence of the Receiver Operating Characteristics of the TT&C Receiver Based on the Dual-Sequence Frequency Hopping

Guangkai Liu, Jie Guo, Weizheng Xin, Cheng Cheng, and Lu Wang

Beijing Institute of Tracking and Telecommunications Technology, Beijing 100094, China

Correspondence should be addressed to Guangkai Liu; dreamer_gk@163.com

Received 22 October 2023; Revised 7 January 2024; Accepted 16 January 2024; Published 27 January 2024

Academic Editor: Fangzhou Fu

Aimed at the antijamming needs of the space tracking, telemetry command (TT&C) receiver under a low signal-to-noise ratio, the anti-interference advantage of the dual-sequence frequency hopping (DSFH) communication system is applied. The channel amplitude fading influence of the receiver operating characteristics (ROC) of the TT&C receiver based on the DSFH is studied. Firstly, based on the typical channel model of the Rayleigh fading without direct path transmission, the conditional Fokker-Planck equation (FPE) is obtained by analyzing the statistical independence of the Rayleigh fading signal and SR output particle moments. Secondly, the probability density function (PDF) of the DSFH signal via channel Rayleigh fading enhanced by stochastic resonance (SR) is obtained by introducing the decision time. Thirdly, the detection probability, false alarm probability, ROC, and system bit error rate (BER) of the DSFH signals enhanced by SR under the Rayleigh fading conditions are obtained, under the minimum BER criterion. Finally, the conclusions are reached: one is that the DSFH signals via channel Rayleigh fading can still be detected by the SR system under low SNR, and the other one is that the SNR can reach the -13 dB by the reception of DSFH signal enhanced by SR, when the Rayleigh fading parameter is 0.2042.

1. Introduction

The space tracking, telemetry and command (TT&C) receiver plays a pivotal role of the connection between the orbiting spacecraft and the ground station which mainly completes the tasks of remote control, telemetry, ranging, and speed measurement. With the intensification of space electromagnetic interference conflicts, the antijamming performance of the TT&C receiver at a low signal-to-noise ratio (SNR) is becoming increasingly urgent [1, 2]. At the same time, under the low SNR, the small-scale fading in the process of space and sky signal transmission has a great impact on the quality of the received signal, thus affecting the antijamming performance of the TT&C receiver. The dual-sequence frequency hopping (DSFH) communication mode uses the idea of "channel is message" [3, 4]. Two groups of pseudorandom sequence-controlled frequency hopping (FH) carrier channels are selected, respectively, through the transmission of symbol 0 or 1. The selected channel is used as the communication channel, while the unselected channel is used as the dual channel. The receiver judges the transmission symbol by detecting the channel occupation [5, 6]. This "dominant modulation" communication mode can effectively combat the tracking interference and other interference patterns and has a certain degree of innate anti-interference performance [7, 8]. Elsayed and Yousif proposed free-space optical (FSO) communication links using the modified pulse-position modulation (MPPM) and spatial pulse-position modulation (SPPM) for reducing the interference and applied the FSO links to UAV to UAV [9–12], which achieved good results. Unlike the traditional communication mode-modulated information in the baseband, the symbol information of DSFH is carried by the presence of RF signals. Therefore, its spatial signal is a single-frequency sine signal, which can be used as the driving signal of the stochastic resonance (SR) system.

SR is a nonlinear physical phenomenon. When the signal, noise, and SR system characteristic are matched, noise

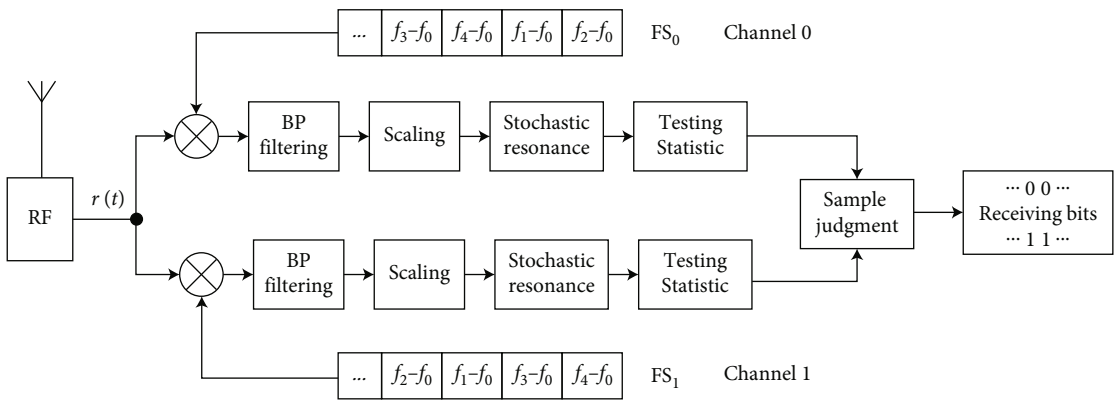

Figure 1: The receiving structure of DSFH enhanced by SR.

plays a positive role in signal detection through the SR system, breaking the traditional view that noise is always harmful in signal detection. Benzi et al. [13] put forward the SR concept in their research on the changes of the Earth's glacial period first, and then, the phenomenon was verified in the fields of physics, biology, and electronics [14–18]. So the SR is used to the signal detection and reception when the signal strength is lower than the decision threshold [19–26]. The output probability density function (PDF) and receiver operating characteristic (ROC) curve of SR driven by an ideal DSFH signal are studied [6, 27]. And the conclusion that SR can be applicable to DSFH signal detection at very low SNR is obtained. However, the signal will inevitably be distorted due to channel transmission, resulting in that the input signal enhanced by the SR system is not an ideal sine signal. But there is little research on the SR output characteristics driven by distorted signals at present.

Aiming at the reception of the DSFH signals via channel fading enhanced by SR, the conditional Fokker-Planck equation (FPE) is obtained by analyzing the statistical independence of the Rayleigh fading signal and particle moments. Then, the output PDF of the signal via the Rayleigh fading enhanced by SR is obtained. Finally, the detection probability, false alarm probability, ROC, and system bit error rate (BER) of the DSFH signals enhanced by SR under the Rayleigh fading conditions are obtained. And the conclusion that the DSFH signal via the Rayleigh fading can be enhanced by the SR system is reached.

2. The System of the Reception of the DSFH Signals via Channel Fading Enhanced by SR

2.1. Subsection. The superheterodyne reception is adopted in the DSFH communication mode, which can be described as shown in Figure 1.

At the radio front (RF), receiving the signal $r(t)$ is mixed and band-pass filtered by the carrier signal controlled by two pseudorandom sequences. The waveform and frequency of the IF signal are the same obtained of the two branches, described as

$$s(t) = A\cos\left[2\pi f_0(t - nT_s) + \varphi\right]\left[\varepsilon(t - nT_s) - \varepsilon(t - (n+1)T_s)\right], \tag{1}$$

where f_0 is the frequency of the IF signal, T_s is the FH period, $\varepsilon(t)$ is the step function, A is the signal amplitude, and φ is the signal phase.

2.2. The Analysis of the SR Output Driven by Random Amplitude Received Signal. The amplitude of the DSFH-received signal is not constant due to the multipath propagation via channel fading, which obeys a certain distribution. At the extremely low SNR, the distribution can be described by Rayleigh, which the amplitude signal is

$$P(A) = \begin{cases} \dfrac{A}{\sigma_A{}^2}\exp\left(-\dfrac{A^2}{\sigma_A{}^2}\right), & A \geq 0 \\ 0, & A < 0 \end{cases}. \tag{2}$$

Then, the SR system driven by the random signal can be represented by Langevin equation (LE) as

$$\frac{dx}{dt} = ax - bx^3 + A\cos(\omega_0 t + \varphi) + n(t), \tag{3}$$

where A is the random amplitude, obeying Rayleigh, and $n(t)$ is the white Gaussian noise.

When A is constant, the relationship between LE and FPE can be obtained by the transition moments of particles and Kramers-Moyal Expansion [22]. So, $\rho(x,t)|A$, which is the probability density function (PDF) of the particle, obeys

$$\frac{\partial\rho(x,t)|A}{\partial t} = -\frac{\partial}{\partial x}\left\{\left[f(x,t) + Dg'(x,t)g(x,t)\right]\rho(x,t)|A\right\} + D\frac{\partial^2}{\partial x^2}\left[g^2(x,t)\rho(x,t)|A\right]. \tag{4}$$

When the signal amplitude A is random, A is dependent of the PDF of the SR output [19]. So the PDF of the SR system is

$$\rho_A(x,t) = \int_{\{A\}} [\rho(x,t)|A]P(A)dA. \tag{5}$$

Further, in order to obtain the particles PDF of the SR system driven by the random signal of $A\cos(\omega_0 t + \varphi)$, the A can be assumed as constant, and then, the conditional PDF as $\rho(x,t)|A$ is obtained. So the $\rho(x,t)$ is carried out at the statistical average according to formula (5).

3. The ROC of SR Driven by DSFH Signal via Channel Fading

3.1. Test Statistics. The test statistics of two hypotheses that the SR system is driven by the DSFH signal and noise or not can be described as

$$\begin{aligned} H_0 &: \quad x(t) = s_{0\_\mathrm{SR}}(t), \\ H_1 &: \quad x(t) = s_{1\_\mathrm{SR}}(t), \end{aligned} \tag{6}$$

where the definite integral is in the form of transcendental function, which can be solved by numerical solution.

$$P[x_0|A\,;H_0] = z_0(t_0)^{-1}\exp\left[-\frac{a^2}{Db}\left(\frac{1}{4}x^4 - \frac{1}{2}x^2\right)\right], \tag{7}$$

$$\begin{aligned} P[x_0|A\,;H_1] = {} & z_1(t_0)^{-1}\exp\left[-\frac{a^2}{Db}\left(\frac{1}{4}x^4 - \frac{1}{2}x^2\right)\right] \\ & \cdot\left\{\exp\left[\sqrt{\frac{a}{D^2b}}xA\cos\left(\frac{\omega_0}{a}t_0 + \varphi\right)\right]\right. \\ & \left. + \exp\left[-\sqrt{\frac{a}{D^2b}}xA\cos\left(\frac{\omega_0}{a}t_0 + \varphi\right)\right]\right\}. \end{aligned} \tag{8}$$

Due to the dependence of the SR and the driven signal, the statistical average of formula (8) is carried out. So the average likelihood function of $x(t)$ under hypothesis of H_1 is

where $s_{0\_\mathrm{SR}}(t)$ is the output signal of the SR system driven by noise singly and $s_{1\_\mathrm{SR}}(t)$ is the output signal of the SR system driven by the DSFH signal and noise.

The decision time t_0 [6], which represents the wave crest and trough of sine signals, is introduced. So the PDF of two hypothesis is

$$\begin{aligned} P[x_0\,;H_1] &= \int_{\{A\}} P[x_0|A\,;H_1]dA \\ &= z_1(t_0)^{-1}\exp\left[-\frac{a^2}{Db}\left(\frac{1}{4}x^4 - \frac{1}{2}x^2\right)\right] \\ &\quad \cdot\int\left\{\exp\left[\sqrt{\frac{a}{D^2b}}xA\cos\left(\frac{\omega_0}{a}t_0 + \varphi\right)\right]\right. \\ &\quad \left. + \exp\left[-\sqrt{\frac{a}{D^2b}}xA\cos\left(\frac{\omega_0}{a}t_0 + \varphi\right)\right]\right\} \\ &\quad \cdot\left[\frac{A}{{\sigma_A}^2}\exp\left(-\frac{A^2}{{\sigma_A}^2}\right)\right]dA. \end{aligned} \tag{9}$$

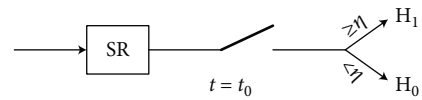

Figure 2: The receiving structure of DSFH after channel fading.

So the likelihood function of the two hypotheses is

$$\begin{aligned} \Lambda(x_0) = \frac{P(x_0|H_1)}{P(x_0|H_0)} = \frac{z_0(t_0)}{z_k(t_0)} \cdot & \int\left\{\exp\left[\sqrt{\frac{a}{D^2b}}xA\cos\left(\frac{\omega_0}{a}t_0 + \varphi\right)\right]\right. \\ & \left. + \exp\left[-\sqrt{\frac{a}{D^2b}}xA\cos\left(\frac{\omega_0}{a}t_0 + \varphi\right)\right]\right\}\left[\frac{A}{{\sigma_A}^2}\exp\left(-\frac{A^2}{{\sigma_A}^2}\right)\right]dA. \end{aligned} \tag{10}$$

The judgment function is

$$\max\{\Lambda(x_0)\} \underset{<}{\geq} \eta, \tag{11}$$

where η is the likelihood ratio decision threshold.

3.2. The Detection Structure under Random Amplitude. The detection structure of the output of the SR system driven by the received IF signal of DSFH after channel fading with the likelihood ratio decision is shown in Figure 2.

3.3. The Performance of Signal Detection. The detection probability with the decision threshold η is

$$\begin{aligned} P_d = \int_\eta P[x_0\,;H_1]dx = z_1(t_0)^{-1}\int_\eta^{+\infty} & \left\{\exp\left[-\frac{a^2}{Db}\left(\frac{1}{4}x^4 - \frac{1}{2}x^2\right)\right]\right. \\ & \cdot\int\left\{\left\{\exp\left[\sqrt{\frac{a}{D^2b}}xA\cos\left(\frac{\omega_0}{a}t_0 + \varphi\right)\right]\right.\right. \\ & \left.\left. + \exp\left[-\sqrt{\frac{a}{D^2b}}xA\cos\left(\frac{\omega_0}{a}t_0 + \varphi\right)\right]\right\}\right. \\ & \left.\left.\cdot\left[\frac{A}{{\sigma_A}^2}\exp\left(-\frac{A^2}{{\sigma_A}^2}\right)\right]\right\}dA\right\}dx. \end{aligned} \tag{12}$$

The false alarm probability is

$$\begin{aligned} P_{fa} &= \int_\eta P[x_0\,;H_0]dx \\ &= z_0(t_0)^{-1}\int_\eta^{+\infty}\exp\left[-\frac{a^2}{Db}\left(\frac{1}{4}x^4 - \frac{1}{2}x^2\right)\right]dx. \end{aligned} \tag{13}$$

The BER is

$$P_e = \frac{1}{2}(1 - P_d) + \frac{1}{2}P_{\mathrm{fa}}. \tag{14}$$

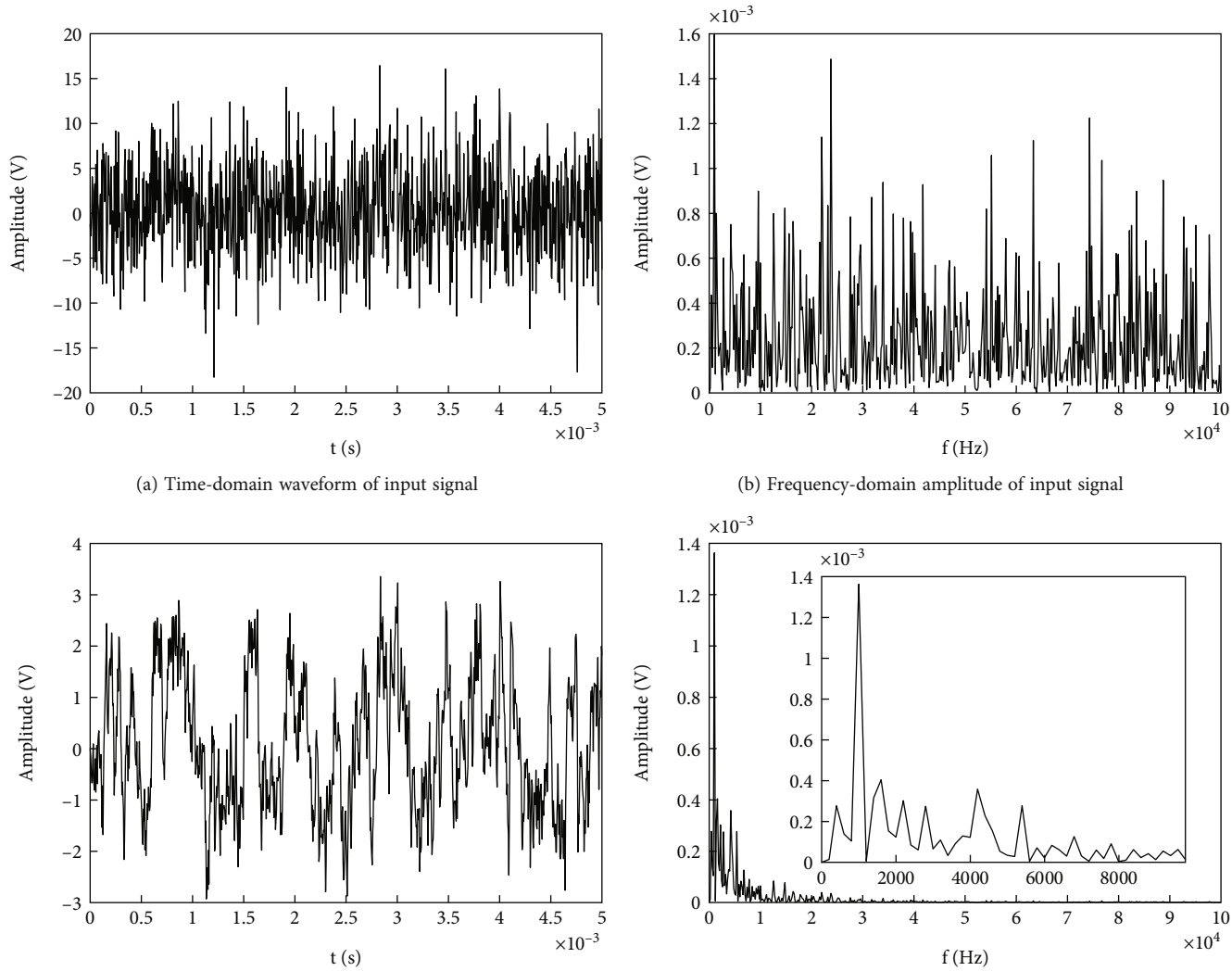

(a) Time-domain waveform of input signal

(b) Frequency-domain amplitude of input signal

(c) Time-domain waveform of output signal

(d) Frequency-domain amplitude of output signal

Figure 3: The waveform of time and frequency zone of sine wave enhanced by SR (input SNR = −14 dB, the noise intensity $\sigma^2 = 4$, and parameters of the system $a = 1 \times 10^4$ and $b = 5.65 \times 10^{12}$).

And the decision threshold η with that the communication system generally adopts the minimum error probability criterion meets

$$\underbrace{\min}_{\eta \in R} P_e. \tag{15}$$

It can be carried out with the necessary conditions for the extreme value of the function

$$\frac{dP_e}{d\eta} = 0. \tag{16}$$

So the numerical solution of η can be obtained with formulas (12)–(14) and (16).

The BER P_e of the SR system driven by DSFH signal via channel fading can be obtained by the numerical solution of η and formula (14).

4. Simulation Results and Discussions

In this section, the theory and simulation are analyzed to demonstrate the detection improvement by the Simulink model of the DSFH signal enhanced by the SR system via channel fading. The simulation parameters are as follows: the frequency of the IF signal is 1 kHz; the sample frequency of the IF signal is 200 kHz; the frequency hopping section is 30-88 kHz; the sample frequency of the RF signal is 2000 kHz.

4.1. The Time-Frequency Characteristic of the DSFH Signals Enhanced by SR via Channel Fading. The IF signal is obtained and processed by superheterodyne demodulated and band-pass filtered of DSFH RF signal which goes through channel fading. Its waveform of time domain and frequency domain is described in Figures 3(a) and 3(b), and its waveform of time domain and frequency domain enhanced by the SR system is described in Figures 3(c) and 3(d). When

the input SNR is -14 dB, its waveform of time domain and frequency domain is disordered and irregular, where there is not any characteristics of IF signal components. However, its waveform of time domain appears periodic characteristics in Figure 3(c) processed by the SR system that it is observed that obvious signal components appear at 1 kHz through the frequency domain in Figure 3(d). From a numerical perspective, the output SNR is -9.4316 dB, raising 4.5684 dB. That is to say, the SNR has improved by 4.5684 dB via the SR system. This is because that enhanced by the SR system, the white Gaussian noise with flat distribution will converge to the low-frequency region, making the energy in the low-frequency region larger. Together with the low-frequency IF signal via the Rayleigh fading, the particles will be driven to transition between the bistable potential wells. The bistable potential wells represent symbols 0 and 1, from a certain perspective. The time-domain signal has a certain periodic characteristic, which is more obvious in the frequency-domain observation. It changes the spectral structure of the noisy signal, which is shown as an increase in SNR on the macrolevel.

4.2. The PDF of the DSFH Signals Enhanced by SR via Channel Fading. The theoretical and simulated PDF $\rho(x, t_0)$ at different positions of the DSFH IF signals enhanced by the SR system via channel fading or not are shown in Figure 4. The PDF $\rho(x, t_0|H_1)$ of the DSFH IF signals enhanced by the SR system is black color, the PDF $\rho(x, t_0|H_1)$ of the DSFH IF signals enhanced by the SR system via channel fading is blue, and the PDF $\rho(x, t_0|H_0)$ of the noise enhanced by the SR system is red. The results show that the driving force of the DSFH IF signal will increase the probability of particles' transition to both sides of the steady state, increasing the residence time of particles in the steady state, increasing the difference between two assumptions, which is more conducive to distinguish between the two hypotheses with the DSFH signal or not and improve the detection probability of DSFH signal. At the same time, compared with the effect of the DSFH IF signal without channel fading, the $\rho(x, t_0|H_1)$ is less different from $\rho(x, t_0|H_0)$. This is because the Rayleigh fading will cause the strength of the DSFH-received signal to decrease, leading to the strength of driving force driving the SR system to decrease, so the difference between the Rayleigh fading and nondriving force will decrease; that is, the Rayleigh fading will weaken the output response of the DSFH signal enhanced by the SR system. It is worth noting that there is a certain gap between theory and simulation. This is because the simulated IF signal always exists, leading to the driving force in the simulation being the comprehensive driving effect of the DSFH signal within one cycle. The black solid line is the output without channel fading. The theoretical value is only related to the driving force state at the current decision time, that is, the time when DSFH has the maximum driving effect, which is quite different from the average driving effect of the simulation. The solid blue line is the average of the Rayleigh fading of the DSFH signal within one cycle, which has little difference with the average driving effect of simulation.

The ROC curves of the DSFH IF signal enhanced by the SR system via channel fading or not are shown in Figure 5. It reflects the relationship between P_d or P_{fa} and the η or SNR, with the black line without channel fading and the red line with channel fading. It can be seen that different ROC curves correspond to different SNR, but they all pass through two points (0,0) and (1,1), which are convex curves located at the upper left of the line of $P_d = P_{\text{fa}}$ with the higher the SNR, the higher the curve position. The signal is better detected, the higher the P_d, with the higher the SNR, when P_{fa} is constant. However, when SNR is constant, the P_d and P_{fa} are decreased with an increase of η. For the detection problem with η known, the tangent point of the slope line of η and the curve is the P_d and P_{fa} with the current SNR and η. At the same time, the detection performance of the red line representing the Rayleigh fading is poorer than the black one without the Rayleigh fading. This is because the Rayleigh fading can decrease the received signal strength and the amplitude, leading to the decrease of the difference between the PDF with the DSFH signal or not. This is also in line with common sense, as the Rayleigh fading affects receiver performance via the SR system. Therefore, the ROC curve can completely describe the likelihood ratio detection performance of the DSFH signal enhanced by the SR system.

The relationship between P_e and SNR of the DSFH IF signal enhanced by the SR system via channel fading or not is shown in Figure 6. It can be seen that the BER of the DSFH signal enhanced by the SR system via the Rayleigh fading is higher than that without fading. This is because the signal strength of the DSFH signal will become smaller and divergent after fading, which will weaken the effect of SR vibration. When SNR is extremely low (SNR < -18 dB without channel fading and SNR < -13 dB with channel fading), the SR system can not get any useful information of DSFH, which is equivalent to random decision, so all four curves are about 0.5. And the SR system gets some useful information of DSFH, when SNR is equal to -18 dB without channel fading where $P_e = 0.4918$. However, the SR system gets some useful information of DSFH via channel fading when the SNR is equal to -13 dB where $P_e = 0.4925$. At the same time, compared with the theory and simulation values of the black one without channel fading, the two curves of the Rayleigh fading have smaller descending speed with SNR. This is because the Rayleigh fading will cause the amplitude of the received signal to diverge, so that the received signal will no longer be a deterministic signal but will become a fluctuating signal, resulting in the same SNR increase and a small increase in BER. Through experiments, it is concluded that DSFH signals via the Rayleigh fading can still be detected and received by the SR system under low SNR. Meanwhile, the Rayleigh fading will reduce the reception performance of the DSFH signals via SR processing. The theoretical boundary of reception performance of the DSFH signals with the Rayleigh fading via SR processing is also obtained. When the fading parameter σ is 0.2042, it is suitable for the reception of the DSFH signals via the Rayleigh fading with SNR > -13 dB. Meanwhile, the Rayleigh fading is mostly applicable to multipath propagation, and there is a direct path in the TT&C communication in most cases, which restricts the applicability of the method.

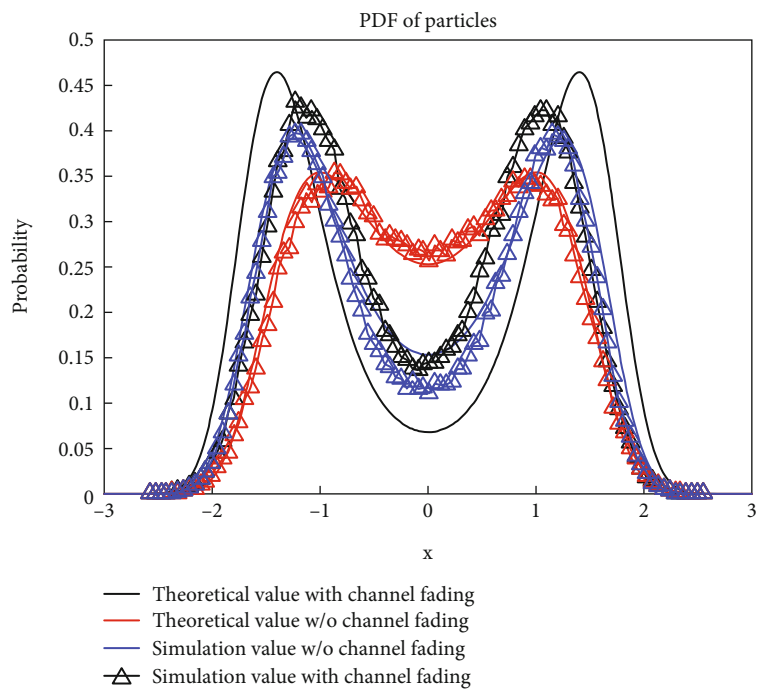

(a)

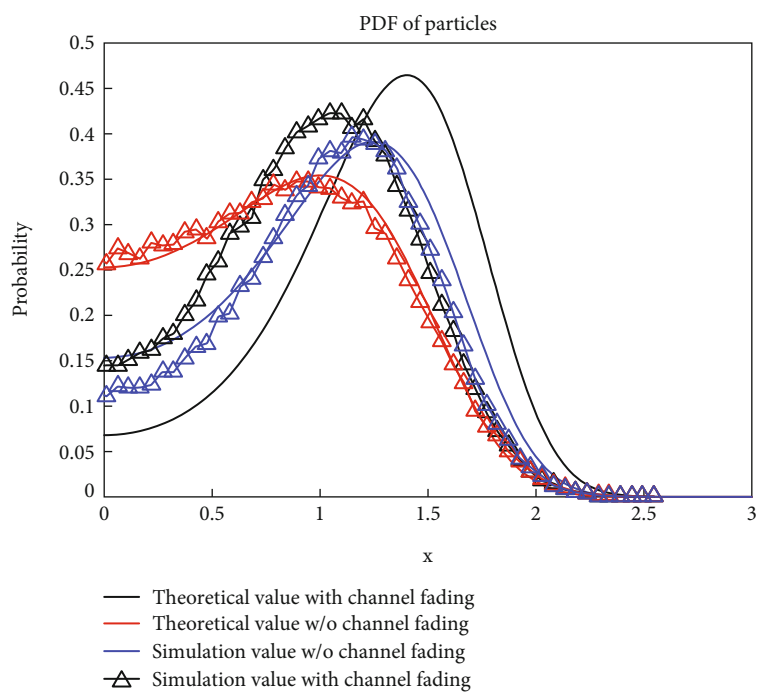

(b)

Figure 4: The PDF of particles of SR (input SNR = −12 dB, the noise intensity $\sigma^2 = 4$, and parameters of system $a = 1 \times 10^4$ and $b = 7.42 \times 10^{12}$).

5. Conclusions

SR can make use of noise to improve the application range of the DSFH signal under extremely low SNR, thereby improving the anti-interference performance of the TT&C receiver using the DSFH system. By analyzing the statistical independence of the Rayleigh fading and moments of SR particles, the receiver performance of the DSFH signal enhanced by the SR system via the Rayleigh fading is obtained. Further, the theoretical boundary of reception performance of the DSFH signals with the Rayleigh fading via SR processing has been obtained. The conclusion that when the fading parameter σ is 0.2042, it is suitable for the reception of the DSFH signals via the Rayleigh fading with SNR > −13 dB

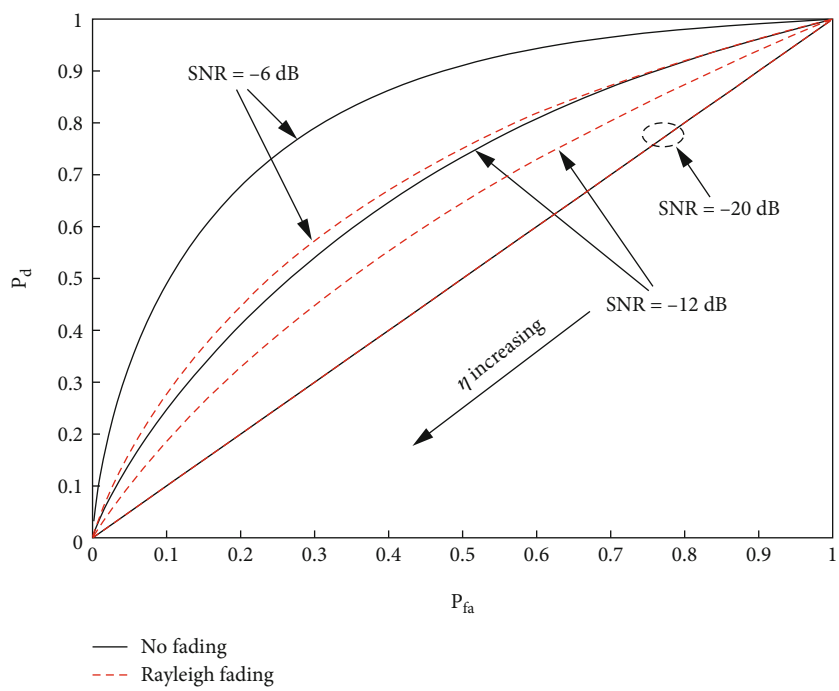

Figure 5: The ROC of the output of SR driven by the DSFH signal.

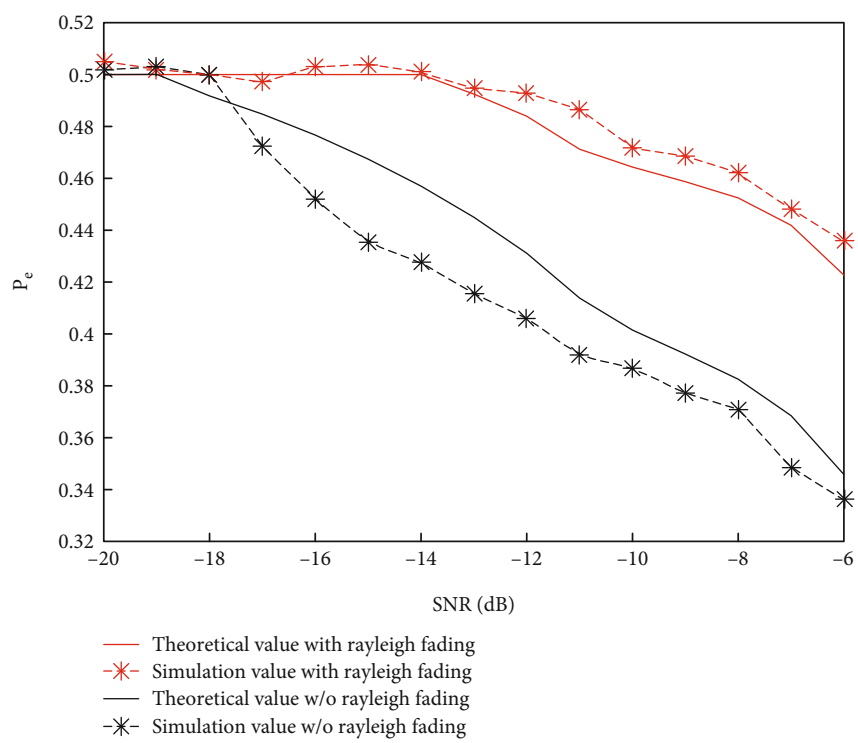

Figure 6: The receiving P_e of SR driven by the DSFH signal.

be obtained. It provides a theoretical support for the practical application of SR in the reception of DSFH signals and provides a reference for the antijamming performance of space TT&C receiver under extremely low SNR. The conclusions can further guide the next experiment. At the same time, by assuming the distortion caused by signal transmission and the statistical independence of SR resonance output moments, the output PDF of SR driven by distorted signals is obtained. The processing method provides a reference for analyzing the influence of distorted signals on SR. Further research focuses on the reception of the DSFH signal via the SR system with a Rice fading.

Data Availability

The data used to support the findings of this study are available from the corresponding or submitting author upon request.

Conflicts of Interest

The authors declare that there is no conflict of interest regarding the publication of this paper.

Funding

The research was funded by the Grant No. 2100050079.

References

[1] B. Giovanni, H. Peter, and V. Enrico, "PN regenerative ranging and its compatibility with telecommand and telemetry signals," *Proceedings of the IEEE*, vol. 95, pp. 2224–2234, 2007.

[2] A. Lavrenko, B. Litchfield, G. Woodward, and S. Pawson, "Design and evaluation of a compact harmonic transponder for insect tracking," *IEEE Microwave and Wireless Components Letters*, vol. 30, no. 4, pp. 445–448, 2020.

[3] F. H. P. Fitzek, "The medium is the message," in *IEEE International Conference on Communications*, pp. 5016–5021, Istanbul, Turkey, 2006.

[4] X. Zhou, P. Kyritsi, and P. C. F. Eggers, ""The medium is the message": secure communication via waveform coding in MIMO systems," in *IEEE Vehicular Technology Conference-vtc-spring*, pp. 491–495, Dublin, Ireland, 2007.

[5] H. D. Quan, H. Zhao, and P. Z. Cui, "Anti-jamming frequency hopping system using multiple hopping patterns," *Wireless Personal Communications*, vol. 81, no. 3, pp. 1159–1176, 2015.

[6] G. K. Liu, H. D. Quan, H. X. Sun, P. Z. Cui, C. Chi, and S. L. Yao, "Stochastic resonance detection method for the dual-sequence frequency hopping signal under extremely low signal-to-noise radio," *Journal of Electronics and Information Technology*, vol. 41, no. 10, pp. 2342–2349, 2019.

[7] H. Zhao, H. D. Quan, and P. Z. Cui, "Follower-jamming resistible multi-sequence frequency hopping wireless communication," *System Engineering and Electronics*, vol. 37, pp. 671–678, 2015.

[8] Y. B. Wang, H. D. Quan, H. X. Cui, and P. Z. Cui, "Anti-follower jamming wide gap multi-pattern frequency hopping communication method," *Defence Technology*, vol. 16, no. 2, pp. 453–459, 2020.

[9] B. Bedir, "Atmospheric turbulence mitigation using spatial mode multiplexing and modified pulse position modulation in hybrid RF/FSO orbital-angular-momentum multiplexed based on MIMO wireless communications system," *Optics Communications*, vol. 436, pp. 197–208, 2019.

[10] E. E. Elsayed and B. B. Yousif, "Performance enhancement of the average spectral efficiency using an aperture averaging and spatial-coherence diversity based on the modified-PPM modulation for MISO FSO links," *Optics Communications*, vol. 463, article 125463, 2020.

[11] E. E. Elsayed and B. B. Yousif, "Performance enhancement of M-ary pulse-position modulation for a wavelength division multiplexing free-space optical systems impaired by interchannel crosstalk, pointing error, and ASE noise," *Optics Communications*, vol. 475, article 126219, 2020.

[12] M. R. Hayal, E. E. Elsayed, D. Kakati et al., "Modeling and investigation on the performance enhancement of hovering UAV-based FSO relay optical wireless communication systems under pointing errors and atmospheric turbulence effects," *Optical and Quantum Electronics*, vol. 55, no. 7, p. 625, 2023.

[13] R. Benzi, A. Sutera, and A. Vulpiani, "The mechanism of stochastic resonance," *Journal of Physics A: Mathematical and General*, vol. 14, no. 11, pp. L453–L457, 1981.

[14] L. Gammaitoni, P. Hänggi, P. Jung, and F. Marchesoni, "Stochastic resonance," *Reviews of Modern Physics*, vol. 70, no. 1, pp. 223–287, 1998.

[15] F. Chapeau-Blondeau and X. Godivier, "Theory of stochastic resonance in signal transmission by static nonlinear systems," *Physical Review E*, vol. 55, no. 2, pp. 1478–1495, 1997.

[16] J. Tougaard, "Signal detection theory, detectability and stochastic resonance effects," *Biological Cybernetics*, vol. 87, no. 2, pp. 79–90, 2002.

[17] Y. M. Kang, "Simulating transient dynamics of the time-dependent time fractional Fokker-Planck systems," *Physics Letters A*, vol. 380, no. 39, pp. 3160–3166, 2016.

[18] S. Wang and F. Z. Wang, "Adaptive stochastic resonance system in terahertz radar signal detection," *Acta Physica Sinica*, vol. 67, no. 16, article 160502, 2018.

[19] P. Krauss, C. Metzner, A. Schilling et al., "Adaptive stochastic resonance for unknown and variable input signals," *Scientific Reports*, vol. 7, no. 1, p. 2450, 2017.

[20] G. K. Liu, H. D. Quan, Y. M. Kang, H. X. Cui, P. Z. Cui, and Y. M. Han, "A quadratic polynomial receiving scheme for sine signals enhanced by stochastic resonance," *Acta Physica Sinica*, vol. 68, article 210501, 2019.

[21] H. D. Quan, G. K. Liu, and H. X. Sun, "A quadratic polynomial receiving scheme for sinusoidal signals enhanced by stochastic resonance under color noise," *IEEE Access*, vol. 99, pp. 63770–63778, 2020.

[22] G. Hu, *Stochastic Forces and Nonlinear Systems*, Shanghai Scientific and Technological Education Publishing House, Shanghai, China, 1994.

[23] S. J. Zhao and J. X. Zhao, *Signal Detection and Estimation Theory*, Publishing House of Electronics Industry, Beijing, China, 2013.

[24] J. Lacik, T. Mikulasek, Z. Raida, and T. Urbanec, "Substrate integrated waveguide monopolar ring-slot antenna," *Microwave and Optical Technology Letters*, vol. 56, no. 8, pp. 1865–1869, 2014.

[25] K. C. Gupta, R. Garg, I. Bahl, and P. Bhartia, *Microstrip Lines and Slotlines*, Artech House, London, UK, 1996.

[26] L. Datashvili and H. Baier, "Derivation of different types of antenna reflectors from the principle of highly flexible structures," in *In proceedings of the 8th European conference on antennas and propagation*, pp. 4–8, Netherlands, the Hague, 2014.

[27] G. K. Liu, Y. Kang, H. D. Quan, H. X. Sun, P. Z. Cui, and C. Guo, "The detection performance of the dual-sequence-frequency-hopping signal via stochastic resonance processing under color noise," *Radioengineering*, vol. 27, no. 3, pp. 618–626, 2019.